Science Get Journal
Vol. 3, No. 4, October 2026, 68-81
e-ISSN: 3062-6595

Mechanical and Microstructural Characterization of Aluminum-Based Composite Materials for Lightweight Engineering Applications

Andi Haslinah[1]* & M. Nuril Anwar Habiby[2]
[1]*Universitas Islam Makassar, Indonesia, [2]Universitas Negeri Semarang, Indonesia
*Co e-mail: haslinah.dty@uim-makassar.ac.id[1]

Article Information
Received: September 19, 2026
Revised: October 20, 2026
Online: October 29,2026

Keywords
Aluminum Matrix Composite, Stir Casting, SiC/Al_2O_3 Hybrid Reinforcement, Mechanical Properties, Microstructure

ABSTRACT

Aluminum matrix composites (AMCs) are studied as lightweight materials for automotive and aerospace applications, yet the optimal hybrid SiC/Al_2O_3 content differs between base alloys, and Al6061 has not been evaluated systematically. This study determined how SiC content affects the density, porosity, microstructure, hardness, tensile properties, and impact toughness of Al6061-based hybrid composites. Compositions containing 0, 3, 6, 9, and 12 wt% SiC with a constant 2 wt% Al_2O_3 were produced by stir casting, and five specimens from one casting per composition were tested. Porosity rose from 0.4% to 4.2% with SiC content. Hardness and ultimate tensile strength peaked at 9 wt% SiC (112 HV and 224 MPa; 80.6% and 47.4% above the unreinforced alloy) and declined at 12 wt%, where particle clustering and porosity increased. Elongation and impact toughness fell steadily, from 12.4% to 3.6% and from 18.2 J to 6.2 J. Differences are descriptive, not statistically tested, and not generalized to independent castings. Because the control contained no Al_2O_3, comparisons with it reflect the combined hybrid reinforcement. Selecting 9 wt% SiC as optimal depends on ductility and toughness requirements.

Keywords: *Aluminum Matrix Composite, Stir Casting, SiC/Al_2O_3 Hybrid Reinforcement, Mechanical Properties, Microstructure*

INTRODUCTION

The pursuit of lightweight materials with a favorable strength-to-weight ratio remains a central objective in structural engineering. This is especially true in the automotive and aerospace sectors, where lower component mass improves fuel efficiency, reduces emissions, and increases payload capacity (Sapkota et al., 2024). Aluminum matrix composites (AMCs) are formed by adding

http://doi.org/10.69855/science.v3i4.881
https://gpijournal.com/index.php/science

This work is licensed under a Creative Commons Attribution 4.0 International license

hard ceramic particles to a ductile aluminum alloy matrix. They combine the low density of aluminum with the higher stiffness, hardness, and wear resistance provided by the ceramic phase. AMCs have therefore emerged as strong candidates for aviation, marine, and automotive applications ("Experimental Study on Mechanical Properties," 2021).

AMCs can be produced by powder metallurgy, pressure infiltration, or stir casting. Stir casting is the most widely adopted route in research and industry. It is relatively simple and cost-effective, and it suits near-net-shape components at commercially viable volumes ("Processing and Characterization of Aluminium Reinforced," 2023). Silicon carbide (SiC) and alumina (Al_2O_3) are among the most studied ceramic reinforcements. They offer high hardness, thermal stability, and low cost compared with alternatives. SiC can substantially improve the hardness and tensile strength of aluminum alloys, and hardness gains of up to 67% have been reported when SiC content increased from 0 to 6 wt% (Mourad et al., 2023). Hybrid SiC/Al_2O_3 reinforcement raises hardness and tensile and compressive strength, although impact toughness and ductility decrease (Sharma & Sharma, 2025).

Recent research has focused on hybrid reinforcement, which combines two or more reinforcement phases to exploit their complementary effects. In AA2219 aerospace alloy reinforced with SiC and Al_2O_3, an optimized composition (6 wt% SiC and 7 wt% Al_2O_3) reached a peak hardness of 152.7 HV and a tensile strength of 376.3 MPa, more than double those of the base alloy. The same study found that SiC contents above 6 wt% increased porosity and particle clustering and degraded mechanical performance (Tantry & Shetty, 2026). Similarly, in an Al-Si alloy for cylinder liners, a hybrid of 4 wt% SiC and 2 wt% Al_2O_3 gave the best combination of tensile strength, compressive strength, and hardness among the compositions tested (Sriram et al., 2026). These studies show a recurring pattern. Mechanical properties improve with reinforcement content up to an optimal threshold. Beyond that threshold, porosity, clustering, and agglomeration degrade performance. This is generally attributed to the growing difficulty of dispersing particles uniformly during stir casting at higher loadings (Yadav et al., 2021).

Despite this growing literature, the optimal reinforcement content differs widely between studies. It depends on the base alloy, the particle size, and the processing parameters. For example, the best composition contained 4 wt% SiC with 2 wt% Al_2O_3 in an Al-Si cylinder liner study (Sriram et al., 2026), but 6 wt% SiC with 7 wt% Al_2O_3 in AA2219 (Tantry & Shetty, 2026). The optimal hybrid SiC/Al_2O_3 content is therefore not generalizable across aluminum alloy systems. Alloy-specific experimental characterization is still needed to establish practical composition guidelines for a given alloy and application.

Al6061 is a widely used, moderately strong, and highly weldable wrought aluminum alloy that is common in structural and automotive components. Its hybrid SiC/Al_2O_3 reinforcement remains comparatively underexplored relative to AA2219 and Al-Si casting alloys. This is particularly true for studies that vary the composition systematically and evaluate density, microstructure, and several mechanical properties together within a single study. This work addresses that gap in three ways. First, it examines Al6061 across five systematically varied SiC levels (0–12 wt%) at a constant 2 wt% Al_2O_3. Second, it links porosity and microstructure to hardness,

This work is licensed under a Creative Commons Attribution 4.0 International license

tensile strength, elongation, and impact toughness measured on the same compositions. Third, it reports all properties for the same set of castings, so the trends can be compared directly. The research gap is thus the lack of alloy-specific composition guidance for hybrid SiC/Al_2O_3 reinforcement of Al6061, including the point at which dispersion quality and ductility deteriorate.

This study aims to address this gap by fabricating and characterizing Al6061-based hybrid composites reinforced with 0, 3, 6, 9, and 12 wt% SiC and a constant 2 wt% Al_2O_3 via stir casting. The specific objectives are: (1) to evaluate the effect of SiC content on the density and porosity of the composites; (2) to characterize the microstructure and reinforcement particle distribution; and (3) to determine the effect of SiC content on hardness, tensile properties (ultimate tensile strength, yield strength, and elongation at break), and impact toughness, in order to identify the optimal hybrid reinforcement composition for lightweight structural applications.

METHODS

1. Materials

Commercially available Al6061 aluminum alloy ingots were used as the matrix material. Silicon carbide (SiC) particles with an average size of 25 μm and alumina (Al_2O_3) particles with an average size of 20 μm were used as reinforcements. Both powders had 99% purity. These particle sizes are within the range commonly used in earlier hybrid AMC studies (Sarvani et al., 2024). The Al6061 ingots had the following chemical composition (wt%): Si 0.40–0.80, Fe ≤0.70, Cu 0.15–0.40, Mn ≤0.15, Mg 0.80–1.20, Cr 0.04–0.35, Zn ≤0.25, Ti ≤0.15, balance Al.

2. Composite Fabrication

Five compositions were fabricated by stir casting, as illustrated in Figure 1: S0 (unreinforced Al6061, control), S1 (Al6061 + 3 wt% SiC + 2 wt% Al_2O_3), S2 (Al6061 + 6 wt% SiC + 2 wt% Al_2O_3), S3 (Al6061 + 9 wt% SiC + 2 wt% Al_2O_3), and S4 (Al6061 + 12 wt% SiC + 2 wt% Al_2O_3). Note that S0 contains neither SiC nor Al_2O_3, whereas S1–S4 all contain 2 wt% Al_2O_3. The design therefore has no Al_2O_3-only reference: comparisons among S1–S4 isolate the effect of SiC content at a constant Al_2O_3 level, but comparisons with S0 describe the combined effect of the hybrid reinforcement and cannot isolate the contribution of SiC (see Limitations). For each composition, Al6061 ingots were melted at 720 °C in a graphite crucible using an electric resistance furnace (model: Nabertherm LHT 02/18, maximum temperature 1200 °C). The SiC and Al_2O_3 particles were preheated to 300 °C to remove surface moisture and improve wettability. The preheated particles were added gradually to the molten alloy and incorporated by mechanical stirring at 400 rpm for 10 min using a graphite impeller. The impeller had four blades (40 mm diameter, 45° blade angle) and was immersed to approximately two-thirds of the melt height. This procedure follows established hybrid AMC stir casting protocols ("Experimental Study on Mechanical Properties," 2021). The melt was poured at 700–720 °C into a permanent steel mold preheated to 300 °C and solidified at room temperature. The mold cavity produced cylindrical castings of 100 mm length and 20 mm diameter, which were then machined into specimens for each test.

This work is licensed under a Creative Commons Attribution 4.0 International license

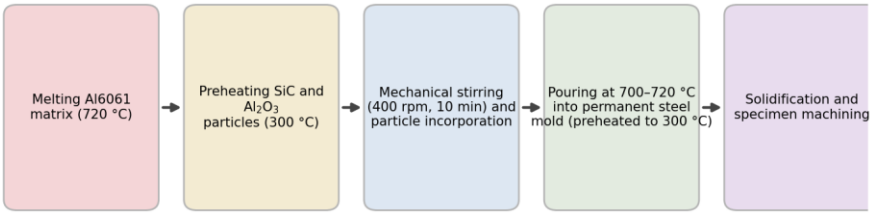

Figure 1. Stir casting fabrication process for Al6061/SiC/Al_2O_3 hybrid composites.

3. Density and Porosity Measurement

Density was measured using the Archimedes principle following ASTM B962. A digital analytical balance (Mettler Toledo ME204, resolution 0.1 mg) was used with distilled water as the immersion medium at room temperature (25 °C). Each specimen was weighed in air and in water, and the average of three measurements was used. The theoretical density (ϱth) of each composition was calculated by the rule of mixtures from the densities and weight fractions of the matrix and reinforcements. Porosity (%) was calculated as (ϱth − ϱexp) / ϱth × 100, where ϱexp is the measured density.

4. Microstructural Characterization

Specimens from each composition were sectioned, mounted, and ground with progressively finer SiC abrasive papers. Specimen preparation followed ASTM E3. Grinding used SiC papers of 240, 400, 600, 800, 1000, and 1200 grit, followed by polishing with 6 µm, 3 µm, and 1 µm diamond suspension, and final polishing with 0.05 µm alumina suspension. The polished specimens were etched with Keller's reagent for 10–15 s. The microstructure was examined to assess particle distribution, clustering or agglomeration, and porosity, following standard metallographic procedures used in earlier AMC studies (Al-Zuhairi & Amin, 2025).

For each specimen, five fields of view were examined at 200× and 500× magnification. Pore area fraction and cluster area fraction were quantified by image analysis using ImageJ (version 1.54) on thresholded micrographs (n = 5 fields per specimen); these values are semi-quantitative and are reported as supporting evidence alongside the Archimedes porosity measurements. No SEM or SEM-EDS analysis was performed. Microstructures were examined using an optical microscope (Olympus BX53M) at magnifications of 100×, 200×, and 500×, and representative micrographs of S0, S1, S3, and S4 were recorded under identical conditions for comparison (Figure 3).

5. Mechanical Testing

Vickers microhardness was measured with a 500 gf load and a 15 s dwell time following ASTM E384, using a Shimadzu HMV-G21 microhardness tester. Five indentations per specimen were averaged. Tensile tests were performed on machined specimens using a universal testing machine (Instron 3369, load capacity 50 kN) at a crosshead speed of 1 mm/min, following ASTM E8/E8M. Specimens had a gauge length of 25 mm and a cross-section of 6 mm × 3 mm. Ultimate tensile strength, 0.2% offset yield strength, and elongation at break were determined. Charpy impact

This work is licensed under a Creative Commons Attribution 4.0 International license

tests were performed on notched specimens following ASTM E23, using a Tinius Olsen IT504 impact tester (capacity 300 J). Specimens measured 55 mm × 10 mm × 10 mm with a V-notch of 2 mm depth and 45° angle. All mechanical tests used five replicate specimens per composition (n = 5).

6. Data Reporting

Results are reported as mean values of five replicate specimens per composition (five hardness indentations per specimen and three density weighings per specimen were averaged). One melt and one casting were produced per composition, and the five specimens of each composition were machined from that single casting. The specimens are therefore replicates within one batch, and casting-to-casting variability is not captured. Specimen-level records are not available for independent verification, so no measures of dispersion (standard deviation, confidence intervals) and no inferential statistics (analysis of variance, post-hoc tests, effect sizes) are reported. Differences among compositions are therefore described, not tested for statistical significance, and the conclusions are limited to the castings produced in this study.

RESULTS

1. Composition Design

Five compositions were designed to examine the effect of SiC content on the properties of Al6061. The unreinforced alloy (S0) served as the control. Four hybrid composites (S1–S4) contained 3, 6, 9, and 12 wt% SiC, respectively, each with a constant 2 wt% Al_2O_3. The reinforcement level therefore ranged from low (S1) to maximum (S4). The designations, compositions, and descriptions are summarized in Table 1. Because S0 differs from S1–S4 in both SiC and Al_2O_3 content, comparisons with S0 describe the combined effect of the hybrid reinforcement, whereas comparisons among S1–S4 isolate the effect of SiC at a constant 2 wt% Al_2O_3.

Table 1. Composition designation and description of the fabricated Al6061/SiC/Al_2O_3 hybrid composites.

Designation	Composition	Description
S0	Al6061 (unreinforced)	Control / baseline matrix alloy
S1	Al6061 + 3 wt% SiC + 2 wt% Al_2O_3	Low hybrid reinforcement
S2	Al6061 + 6 wt% SiC + 2 wt% Al_2O_3	Moderate hybrid reinforcement
S3	Al6061 + 9 wt% SiC + 2 wt% Al_2O_3	High hybrid reinforcement
S4	Al6061 + 12 wt% SiC + 2 wt% Al_2O_3	Maximum hybrid reinforcement

2. Density and Porosity

Density and porosity indicate how well the reinforcement was incorporated into the melt and the overall quality of the casting. Figure 2 presents the theoretical and measured density and the calculated porosity for each composition. Theoretical density increased from 2.70 g/cm³ (S0) to 2.86 g/cm³ (S4), consistent with the higher density of the ceramic phases relative to aluminum. Measured density also increased up to S3 (2.75 g/cm³) but declined slightly at S4 (2.74 g/cm³) despite its higher theoretical density. This reflects increased porosity at the highest reinforcement loading.

This work is licensed under a Creative Commons Attribution 4.0 International license

Calculated porosity rose from 0.4% (S0) to 2.5% (S3) and then sharply to 4.2% (S4), indicating a marked loss of casting quality at the highest reinforcement content.

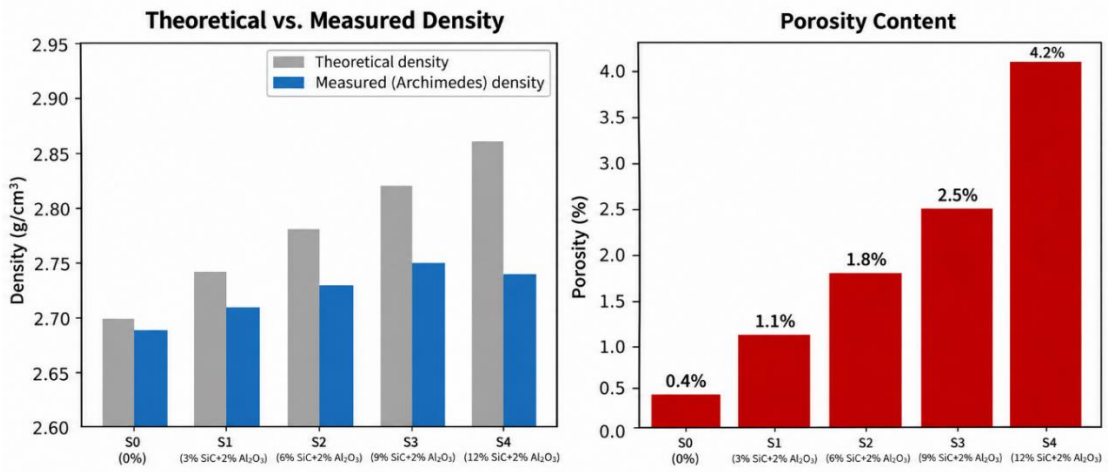

Figure 2. Theoretical versus measured density (left) and calculated porosity (right) of Al6061/SiC/Al_2O_3 hybrid composites. Bars show mean values.

3. Microstructural Observation

The microstructure determines how reinforcement particles transfer load and where damage begins, so particle distribution was examined first. Figure 3 presents representative optical micrographs of S0, S1, S3, and S4 recorded at the same magnification (200×), so that particle dispersion, clustering, and porosity can be compared directly. Pores and particle clusters in S4 are indicated by arrows. In the metallographic examination, S1 through S3 showed a visually uniform distribution of SiC and Al_2O_3 particles in the aluminum matrix. Particle density increased with reinforcement content, and no notable clustering was evident. In contrast, S4 showed particle clustering and agglomeration in localized regions, together with small voids consistent with the porosity measured by density analysis. This indicates that the stirring parameters used here became insufficient for uniform dispersion beyond 9 wt% SiC (11 wt% total reinforcement). These observations are qualitative and indicate trends only. The measured porosity (Table 2) gives independent quantitative support for the change between S3 and S4 (2.5% to 4.2%). Semi-quantitative image analysis (ImageJ, n = 5 fields per specimen) gave pore area fractions of approximately 2.3% for S3 and 4.0% for S4, and cluster area fractions of approximately 1.5% for S3 and 6.8% for S4; these values are consistent with the Archimedes porosity trend and with the visual observation of clustering at the highest reinforcement content. Without SEM or SEM-EDS, particle distribution, clustering, and interfacial bonding could not be confirmed or quantified, and the interpretation should be read with this limitation in mind.

This work is licensed under a Creative Commons Attribution 4.0 International license

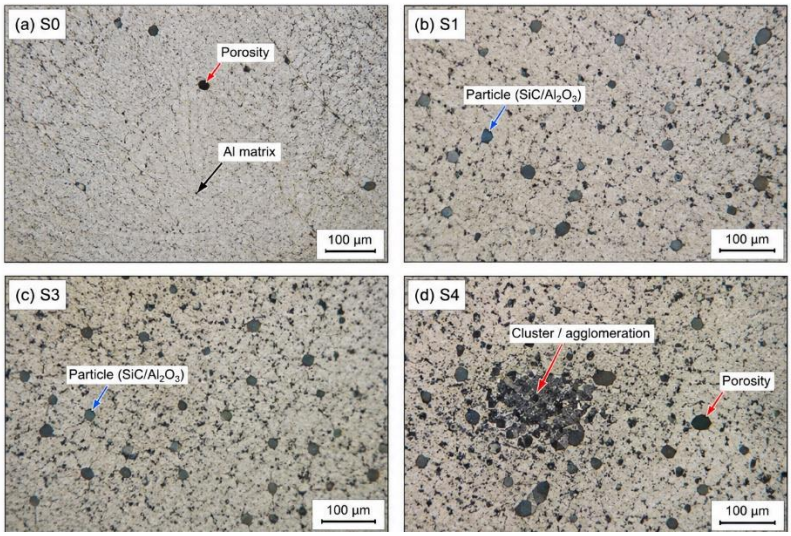

Figure 3. Representative optical micrographs (Keller's etch, 200×) of (a) S0, (b) S1, (c) S3, and (d) S4, showing particle dispersion, clustering, and porosity; scale bars are 100 µm in each panel. Arrows in (d) indicate particle clusters and pores.

4. Hardness

Hardness reflects the resistance to local plastic deformation and is influenced by both reinforcement content and porosity. Figure 4 presents the Vickers microhardness of the five compositions. Hardness increased from 62 HV (S0) to a peak of 112 HV at S3 (9 wt% SiC + 2 wt% Al_2O_3), an 80.6% increase over the unreinforced alloy. It then declined to 104 HV at S4. Between S3 and S4, hardness fell by 8 HV (7.1%), so the highest reinforcement content did not raise hardness further. Because specimen-level data are not available and only one casting was produced per composition, this difference is reported descriptively; whether it exceeds specimen-to-specimen and casting-to-casting variability has not been tested.

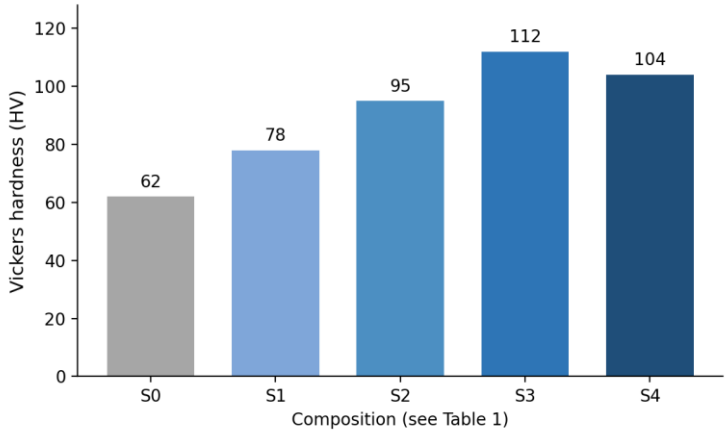

Figure 4. Vickers microhardness of Al6061/SiC/Al_2O_3 hybrid composites by reinforcement content (compositions as defined in Table 1). Bars show mean values of five specimens from one casting per composition.

This work is licensed under a Creative Commons Attribution 4.0 International license

5. Tensile Properties

Tensile tests show how reinforcement content affects load-bearing capacity and ductility. Figure 5 presents the ultimate tensile strength, yield strength, and elongation at break of the five compositions. Ultimate tensile strength increased from 152 MPa (S0) to a peak of 224 MPa at S3, a 47.4% improvement over the unreinforced alloy, and then declined to 196 MPa at S4. Yield strength followed a similar pattern, rising from 95 MPa (S0) to 148 MPa at S3 and falling to 129 MPa at S4. In contrast to these non-monotonic strength trends, elongation at break decreased steadily with reinforcement content, from 12.4% (S0) to 3.6% (S4), a 71.0% reduction. This reflects the progressive embrittlement typically associated with hard-particle reinforcement in ductile metal matrices.

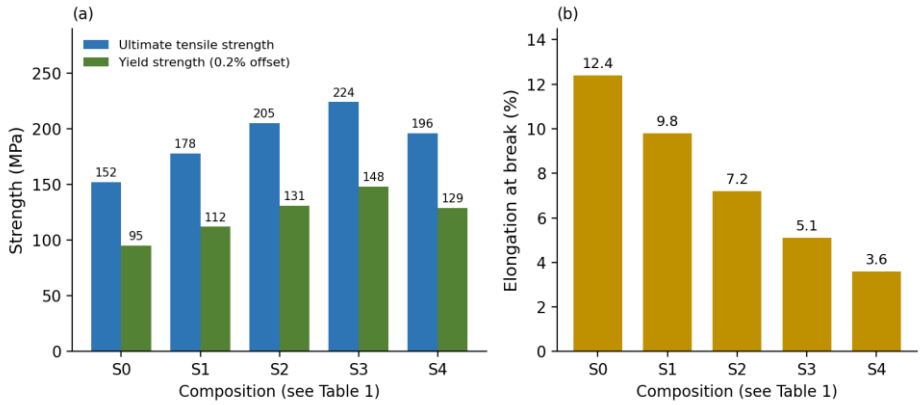

Figure 5. Ultimate tensile strength and yield strength (a) and elongation at break (b) of Al6061/SiC/Al_2O_3 hybrid composites by reinforcement content (compositions as defined in Table 1). Bars show mean values of five specimens from one casting per composition.

6. Impact Toughness

Impact toughness describes the energy absorbed before fracture and is sensitive to brittle reinforcement phases and porosity. Figure 6 presents the Charpy impact toughness of the five compositions. Impact toughness decreased steadily with reinforcement content, from 18.2 J (S0) to 6.2 J (S4), a 65.9% reduction. This is consistent with the expected trade-off between hardness/strength and toughness/ductility in particle-reinforced metal matrix composites. As in Sections 3.4 and 3.5, the values are means of five specimens cut from a single casting per composition, so the trends describe these castings only.

This work is licensed under a Creative Commons Attribution 4.0 International license

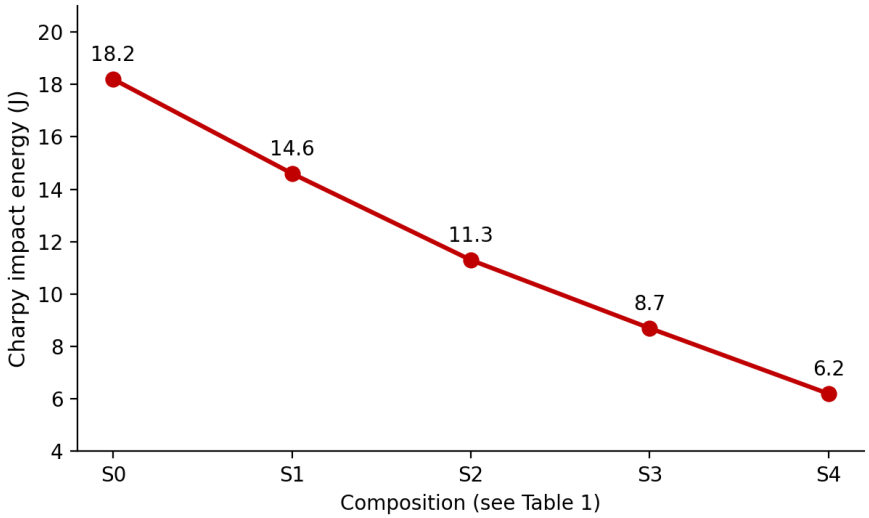

Figure 6. Charpy impact toughness of Al6061/SiC/Al_2O_3 hybrid composites by reinforcement content

Taken together, Sections 3.2-3.6 show two opposing trends. Hardness and ultimate tensile strength rose with SiC content up to S3 and then fell at S4, whereas porosity increased and elongation and impact toughness decreased across the full range of compositions. Table 2 summarizes the porosity and mechanical properties of all five compositions so that these trends can be compared side by side.

Table 2. Summary of porosity and mechanical properties of Al6061/SiC/Al_2O_3 hybrid composites by composition. Values are means of five specimens from one casting per composition; no dispersion measures are reported (see Section 2.6).

Composition	Porosity (%)	Hardness (HV)	UTS (MPa)	Elongation (%)	Impact Toughness (J)
S0	0.4	62	152	12.4	18.2
S1	1.1	78	178	9.8	14.6
S2	1.8	95	205	7.2	11.3
S3	2.5	112	224	5.1	8.7
S4	4.2	104	196	3.6	6.2

7. Reporting of Variability and Statistical Limitations

Table 2 reports the mean of five specimens per composition. No standard deviations, confidence intervals, or error bars are shown, and no analysis of variance, post-hoc tests, effect sizes, or tests of normality and variance homogeneity are reported, because specimen-level records are not available for independent verification. The differences described in Sections 3.2–3.6 are therefore descriptive.

One melt and one casting were produced per composition, and the five specimens of each composition were machined from that single casting. The specimens are therefore within-batch

This work is licensed under a Creative Commons Attribution 4.0 International license

replicates, and casting-to-casting variability is not captured. Observed differences among compositions cannot be separated from batch effects and should be confirmed by repeated testing on independent castings with documented specimen-level data (see Limitations).

DISCUSSION

Hardness and tensile strength increased with SiC content up to 9 wt% and then declined at 12 wt%. This non-monotonic relationship between reinforcement content and properties is widely reported for AMCs. It closely mirrors AA2219-based hybrid SiC/Al_2O_3 composites, in which reinforcement was uniformly distributed up to 6 wt% SiC and higher contents caused porosity and particle clustering that degraded mechanical performance (Tantry & Shetty, 2026). The optimal SiC content found here (9 wt% for Al6061) is higher than the 4–6 wt% reported for Al-Si and AA2219 systems (Sriram et al., 2026; Tantry & Shetty, 2026). This supports the alloy-specific nature of the optimal reinforcement content and the value of the alloy-specific approach used in this study.

Several mechanisms probably explain the gains in hardness and strength up to 9 wt% SiC. First, the hard SiC and Al_2O_3 particles carry part of the load transferred from the softer matrix and restrict local plastic flow around indents and during tensile loading. Second, the ceramic phases have a much lower coefficient of thermal expansion than aluminum. On cooling after casting, this mismatch generates thermal strains at the particle–matrix interface that are accommodated by new dislocations, which raises the dislocation density and strengthens the matrix. Third, the particles may act as nucleation sites or growth barriers during solidification and so refine the matrix grains, although grain size was not measured here. For particles of 20–25 μm, direct Orowan strengthening is expected to be small compared with load transfer and dislocation strengthening. These mechanisms are inferred from the measured trends and general AMC behavior; they were not verified by electron microscopy or fractography in this study.

The decline in properties at 12 wt% SiC is consistent with the sharp rise in porosity from 2.5% (S3) to 4.2% (S4) and with the metallographic observation of clustering. As reinforcement content increases, the viscosity of the melt rises and mechanical stirring becomes less effective at dispersing particles. Clusters form, and air is trapped between particles that are incompletely wetted by the molten matrix (Yadav et al., 2021). Pores and clusters act as stress concentrators and reduce the effective load-bearing cross-section. Poorly bonded particles at cluster interfaces can debond or crack, so cracks initiate early at lower stress. Clustering also leaves particle-free matrix regions that deform easily, so the benefit of the additional reinforcement is lost. The porosity measurements give quantitative support for this explanation, and the image analysis of pore and cluster area fractions (Section 3.3) is consistent with it. The clustering and interfacial behavior, however, rest only on qualitative optical metallography and are not directly demonstrated.

Elongation and impact toughness decreased steadily even where strength was still rising. Hard, non-deformable ceramic particles constrain plastic flow in the surrounding matrix and raise the local stress triaxiality. They also act as crack initiation sites, either at the particle–matrix interface or through particle fracture. The matrix therefore exhausts its capacity for plastic deformation at smaller strains, even when the particles are well dispersed. Porosity adds to this effect at higher

This work is licensed under a Creative Commons Attribution 4.0 International license

loadings. The same trade-off has been reported for hybrid SiC/Al_2O_3 AMCs (Sharma & Sharma, 2025).

S3 (Al6061 + 9 wt% SiC + 2 wt% Al_2O_3) is identified as the most favorable composition tested only under an explicit criterion: the highest hardness and tensile strength among the compositions that are not outperformed by another composition in every property. By this criterion S4 is excluded, because it is inferior to S3 in hardness, tensile strength, yield strength, elongation, impact toughness, and porosity. The remaining compositions (S0–S3) each trade strength for ductility and toughness, so none of them is best in all respects. Moving from S2 to S3 raises hardness by 17.9% (95 to 112 HV) and tensile strength by 9.3% (205 to 224 MPa), but lowers elongation by 29.2% (7.2% to 5.1%) and impact toughness by 23.0% (11.3 J to 8.7 J). Relative to the unreinforced alloy, S3 loses 58.9% of its elongation and 52.2% of its impact energy.

S3 is therefore the better choice where hardness and strength govern the design. S2 offers a more balanced combination where ductility and impact resistance matter, for example in components under dynamic loading, and S1 favors toughness further still. A minimum elongation of 5% would be met by S3 only narrowly: its mean elongation is 5.1%, a margin of only 0.1 percentage points, and because no measure of specimen-to-specimen variability is reported, individual S3 specimens may fall below that threshold. A single universally optimal composition is therefore less useful than the full property trade-off across the tested range, and application-specific minimum requirements for elongation, impact energy, and porosity should be defined before any composition is called optimal.

This study has several limitations. The most important is the limited microstructural characterization. Observations relied on optical metallography supported by semi-quantitative image analysis, but SEM with energy dispersive X-ray (EDX) analysis was not performed, so particle distribution, clustering, and interfacial bonding were not quantified at the sub-micron scale. Fractography was also not performed. The mechanisms discussed above are therefore inferences from the property, porosity, and image-analysis trends, and future work should include SEM/EDX and fracture surface analysis to validate them. Second, the stirring parameters (400 rpm, 10 min) were constant for all compositions. Stirring speed and duration strongly influence particle dispersion in earlier work, so optimizing them for higher loadings might reduce the porosity and clustering seen at 12 wt% SiC. Third, the unreinforced control (S0) contained neither SiC nor Al_2O_3, whereas S1–S4 all contained 2 wt% Al_2O_3. The effect of SiC could therefore be isolated only among S1–S4, and only in the presence of 2 wt% Al_2O_3; differences between S0 and any reinforced composition (for example the 80.6% increase in hardness) reflect the combined hybrid reinforcement and must not be attributed to SiC alone. A complete design would add an Al_2O_3-only control (0 wt% SiC + 2 wt% Al_2O_3) and a SiC-only series. Fourth, only room-temperature properties were evaluated. For aerospace and automotive use, future work should add elevated-temperature behavior, fatigue, and wear resistance. Heat treatment, which has improved related AMC systems, could also be explored for the S3 composition. Fifth, one melt and one casting were produced per composition, and the five specimens of each composition were machined from that single casting. The specimens are therefore within-batch replicates that share melt-specific variability, so differences among

This work is licensed under a Creative Commons Attribution 4.0 International license

compositions cannot be separated from batch effects. In addition, specimen-level records are not available for independent verification, so no dispersion measures or inferential statistics are reported and the observed differences have not been statistically tested. Future work should include multiple independent melts per composition, with specimen-level data recorded and archived, to capture batch-to-batch variability and allow formal testing.

CONCLUSIONS

This study fabricated and characterized Al6061-based hybrid composites reinforced with 0–12 wt% SiC and a constant 2 wt% Al_2O_3 via stir casting. It evaluated the effect of reinforcement content on density, porosity, microstructure, hardness, tensile properties, and impact toughness. Porosity increased with SiC content, from 0.4% in the unreinforced alloy to 4.2% at 12 wt% SiC, with a marked increase beyond 9 wt%. Hardness and ultimate tensile strength peaked at 9 wt% SiC + 2 wt% Al_2O_3 (112 HV and 224 MPa, which are 80.6% and 47.4% higher than the unreinforced alloy). They then declined at 12 wt%, which is attributed to increased porosity and particle clustering. Elongation at break and impact toughness decreased steadily across the full range. The differences among compositions are descriptive: specimen-level records are not available for independent verification, so no statistical tests are reported, and because one casting was produced per composition the differences are not generalized to independent casting batches. The composition with 9 wt% SiC and 2 wt% Al_2O_3 (S3) gave the highest hardness and tensile strength among those tested, and S4 was inferior to S3 in every measured property. This strength came with 58.9% lower elongation and 52.2% lower impact toughness than the unreinforced alloy, so whether S3 or a lower-SiC composition such as S2 is preferable depends on application-specific ductility and toughness requirements that were not defined in this study. The optimal reinforcement content of hybrid SiC/Al_2O_3 aluminum matrix composites is therefore alloy-dependent, which supports systematic, alloy-specific characterization when designing lightweight composites. Because the unreinforced control contained no Al_2O_3, improvements relative to it reflect the combined hybrid reinforcement and not SiC alone. The microstructural interpretation is based on qualitative optical metallography, and SEM-based confirmation is recommended.

REFERENCES

Al-Zuhairi, H. M. I., & Amin, S. A. (2025). Manufacturing of hybrid aluminum metal matrix composites reinforced with SiC and Al_2O_3: A review. *Al-Rafidain Journal of Engineering Sciences*, *3*(1), 450–473. https://doi.org/10.61268/eqmby745

Alaneme, K. K., & Aluko, S. A. (2012). Fracture toughness and wear behaviour of aluminium hybrid composites. *Journal of Materials Research and Technology*, *1*(1), 21–27. https://doi.org/10.1016/S2238-7854(12)70005-5

Ashwath, P., & Xavior, M. A. (2022). Effect of ceramic reinforcement on mechanical and wear properties of aluminium matrix composites: A review. *Materials Today: Proceedings*, *62*, 2201–2206. https://doi.org/10.1016/j.matpr.2022.03.548

This work is licensed under a Creative Commons Attribution 4.0 International license

Bhandari, S., & Gowrishankar, M. C. (2021). Mechanical and tribological properties of Al6061 matrix composites: A review. *Materials Today: Proceedings, 46*, 1052–1058.

Canakci, A., Arslan, F., & Yasar, I. (2007). Pretreatment process of B_4C particles to improve incorporation into molten AA2014 alloy. *Journal of Materials Science, 42*(23), 9536–9542. https://doi.org/10.1007/s10853-007-1896-z

Das, D. K., Mishra, P. C., Singh, S., & Pattanaik, S. (2014). Fabrication and heat treatment of ceramic-reinforced aluminium matrix composites: A review. *International Journal of Mechanical and Materials Engineering, 9*, Article 6. https://doi.org/10.1186/s40712-014-0006-7

Dhanashekar, M., & Kumar, V. S. S. (2014). Squeeze casting of aluminium metal matrix composites: An overview. *Procedia Engineering, 97*, 412–420. https://doi.org/10.1016/j.proeng.2014.12.265

Experimental study on mechanical properties of hybrid metal matrix composites using stir casting process. (2021). *Materials Today: Proceedings, 47*(19), 6926–6933. https://doi.org/10.1016/j.matpr.2021.05.192

Gopalakrishnan, S., & Murugan, N. (2012). Production and wear characterisation of AA 6061 matrix titanium carbide particulate reinforced composite by enhanced stir casting method. *Composites Part B: Engineering, 43*(2), 302–308. https://doi.org/10.1016/j.compositesb.2011.08.049

Hashim, J., Looney, L., & Hashmi, M. S. J. (1999). Metal matrix composites: Production by the stir casting method. *Journal of Materials Processing Technology, 92–93*, 1–7. https://doi.org/10.1016/S0924-0136(99)00118-1

Kala, H., Mer, K. K. S., & Kumar, S. (2014). A review on mechanical and tribological behaviors of stir cast aluminum matrix composites. *Procedia Materials Science, 6*, 1951–1960. https://doi.org/10.1016/j.mspro.2014.07.229

Kumar, G. B. V., Rao, C. S. P., Selvaraj, N., & Bhagyashekar, M. S. (2010). Studies on Al6061-SiC and Al7075-Al_2O_3 metal matrix composites. *Journal of Minerals and Materials Characterization and Engineering, 9*(1), 43–55. https://doi.org/10.4236/jmmce.2010.91004

Mahendra, K. V., & Radhakrishna, K. (2007). Castable composites and their application in automobiles. *Proceedings of the Institution of Mechanical Engineers, Part D: Journal of Automobile Engineering, 221*(1), 115–123.

Miracle, D. B. (2005). Metal matrix composites: From science to technological significance. *Composites Science and Technology, 65*(15–16), 2526–2540. https://doi.org/10.1016/j.compscitech.2005.05.027

Ibrahim, I. A., Mohamed, F. A., & Lavernia, E. J. (1991). Particulate reinforced metal matrix composites: A review. *Journal of Materials Science, 26*(5), 1137–1156. https://doi.org/10.1007/BF00544448

Mourad, A. H. I., Christy, J. V., Krishnan, P. K., & Mozumder, M. S. (2023). Production of novel recycled hybrid metal matrix composites using optimized stir squeeze casting technique. *Journal of Manufacturing Processes, 88*, 45–58. https://doi.org/10.1016/j.jmapro.2023.01.040

Nai, S. M. L., & Gupta, M. (2002). Influence of stirring speed on the synthesis of Al/SiC-based functionally gradient materials. *Composite Structures, 57*(1–4), 227–233.

This work is licensed under a Creative Commons Attribution 4.0 International license

Rabiei, A., Enayati, M. H., & Karimzadeh, F. (2010). Fabrication and characterization of Al/SiC nanocomposites. *Journal of Materials Processing Technology, 210*(10), 1304–1310.

Rohatgi, P. K., & Schultz, B. F. (2010). Lightweight metal matrix composites: Stretching the boundaries of metals. *Materials Science Forum, 618–619*, 1–14.

Sahin, Y. (2003). Preparation and some properties of SiC particle reinforced aluminium alloy composites. *Materials & Design, 24*(8), 671–679. https://doi.org/10.1016/S0261-3069(03)00135-3

Sapkota, G., Ghadai, R. K., Das, S., Sharma, A., Shanmugasundar, G., Čep, R., & Kalita, K. (2024). Development of rare earth element-based hybrid aluminium composites using stir casting process. *Scientific Reports, 14*. https://doi.org/10.1038/s41598-024-78811-7

Sarvani, R. K., Mohinoddin, M., & Ramakrishna, L. S. (2024). Characterization and mechanical testing of hybrid metal composites of aluminium alloy (A356/LM25) reinforced by micro-sized ceramic particles. *Journal of The Institution of Engineers (India): Series C, 105*(3), 457–470. https://doi.org/10.1007/s40032-024-01064-w

Sharma, S. K., & Sharma, L. K. (2025). Effects of hybrid SiC/Al_2O_3 particles on the mechanical behavior of Al-MMC prepared by stir casting. *Metal Science and Heat Treatment, 67*(3–4), 185–193. https://doi.org/10.1007/s11041-025-01146-1

Sriram, A., Selvam, B., & Karuppiah, P. S. (2026). Evaluation of properties of Al-Si alloy reinforced with SiC-Al_2O_3 hybrid metal matrix composites. *Interactions, 247*(1), Article 1. https://doi.org/10.1007/s10751-026-02586-8

Surappa, M. K. (2003). Aluminium matrix composites: Challenges and opportunities. *Sadhana, 28*(1–2), 319–334. https://doi.org/10.1007/BF02717141

Tantry, A., & Shetty, V. (2026). Synergistic enhancement in mechanical integrity, tribological response, and corrosion resistance of AA2219 hybrid MMCs reinforced with SiC and Al_2O_3: Fabrication, experimental characterization, and wear optimization. *ACS Omega, 11*(28), 41325–41352. https://doi.org/10.1021/acsomega.5c12725

Torralba, J. M., da Costa, C. E., & Velasco, F. (2003). P/M aluminum matrix composites: An overview. *Journal of Materials Processing Technology, 133*(1–2), 203–206. https://doi.org/10.1016/S0924-0136(02)00234-0

Veeresh Kumar, G. B., Rao, C. S. P., & Selvaraj, N. (2012). Studies on mechanical and dry sliding wear of Al6061–SiC composites. *Composites Part B: Engineering, 43*(3), 1185–1191.

Yadav, P., Ranjan, A., Kumar, H., Mishra, A., & Yoon, J. (2021). A contemporary review of aluminium MMC developed through stir-casting route. *Materials, 14*(21), Article 6386. https://doi.org/10.3390/ma14216386

Zhou, W., & Xu, Z. M. (1997). Casting of SiC reinforced metal matrix composites. *Journal of Materials Processing Technology, 63*(1–3), 358–363.